Modelling the autoxidation of myoglobin in fresh meat under modified atmosphere packing conditions

J. Tofteskov[*], J.S. Hansen, N.P. Bailey

Department of Science and Environment, Roskilde University, P.O. Box 260, DK-4000, Roskilde, Denmark

A B S T R A C T

Modified atmosphere packing (MAP) is a technique to increase the shelf life of fresh meat. Continuing development of MAP requires better understanding of the physical and chemical processes taking place, in particular the diffusion of oxygen and its reaction with myoglobin. We model these processes using reaction-diffusion equations. The reactions include binding of oxygen to myoglobin, oxidation of myoglobin and other oxygen consuming processes. Model parameters have been extrapolated using data from the literature to relevant temperatures and pH values. Partial agreement with spatially resolved pigment concentration data is obtained, but only by substantially increasing the value of the oxygen consumption rate. Application of the model to meat stored at 5 °C shows that the metmyoglobin layer forms under the surface over a time scale of 24 h; The metmyoglobin layer forms deeper inside the meat proportional to the logarithm of the headspace oxygen partial pressure, thus improving the colour appearance of the meat.

© 2017 Elsevier Ltd. All rights reserved.

1. Introduction

Increased shelf life of foods is important for economic and environmental reasons because it can potentially reduce the amount of waste (Wikström et al., 2014). Fresh meat is often packed and stored prior to consumption using modified atmospheric packaging (MAP) in which the meat is packed in an atmosphere of, normally, 80% O_2. The oxygen binds to the tissue myoglobin, Mb, to produce oxymyoglobin, MbO_2. Also oxidation of Mb or MbO_2 produces metmyoglobin, MMb; this oxidation is referred to as autoxidation. In this state the meat becomes brown, which is not attractive to consumers. In fresh meat one can often observe a brown layer of MMb expanding outwards from inside the meat, as described by Sáenz et al. (2008). Colour stability is a major concern as MAP technology continues to be developed (McMillin, 2008). Possible future developments include the use of active packaging, reducing the headspace, and tuning the MAP parameters (barrier materials, gas composition) to specific meat products. In connection with such development there is a clear need for more data on the various processes taking place in fresh meat stored under MAP for different conditions (McMillin, 2008). It is also becoming clear

that mathematical modelling can play an important role in such development (Riva et al., 2009). In this work we present a model for diffusion of oxygen and its reactions in meat; special focus is on reactions with myoglobin.

Oxygen has to diffuse into the meat before reactions can occur. Moreover, the concentration of Mb in meat is on the order of that of oxygen under air-saturated conditions, at least for beef (Chaix et al., 2014), and thus binding to myoglobin together with other oxygen consuming processes such as mitochondrial respiration are enough to significantly slow down the advance of oxygen. We have a situation where the types of processes— oxygen diffusion and its chemical reactions—affect each other strongly and must both be included in a model; here we shall be using a reaction-diffusion system. Sáenz et al. (2008) made a simple reaction-diffusion model to help interpret their measurements of concentration profiles of myoglobin in different states. Their linear model involved only O_2 and Mb as dynamical variables, and included the reversible binding of oxygen to Mb, known as oxygenation, but not autoxidation of Mb.

The redox chemistry of myoglobin is complicated. This is reflected in how the oxidation rate depends non-trivially on pH and the local O_2 concentration, as well as the type of myoglobin; the latter varies not just from one biological species to another, but also from one muscle type to another in the same species. Temperature dependence is also important, and must be addressed

---

appropriately. While we consider the situation where temperature and pH are constant, the O_2 concentration will vary in space and time and this must be explicitly modelled. Some attention to temperature and pH dependence must be given; much of the data on the reaction mechanisms, and associated kinetic parameters, have been obtained for physiological conditions (37 °C, pH $\simeq$ 7) or at room temperature, while fresh meat is usually stored around 5 °C and has a lower pH, typically near 5.5–5.7, though this depends on processing conditions post mortem (Owusu-Apenten, 2004).

The oxygen dependence of the autoxidation of myoglobin was investigated by George and Stratmann (1952) who found a non-monotonic oxidation rate for native bovine myoglobin rising from zero at zero O_2 concentration, reaching a maximum at around 4 μM of dissolved oxygen, before converging towards a lower rate at large concentrations of O_2. This non-monotonic behaviour suggests that some non-linear reaction mechanism is involved. The existence of a maximum at relative low O_2 concentrations provides a mechanism for why the MMb layer appears first under the surface of the meat. There have been many attempts in the literature to identify a molecular mechanism for the autoxidation which can explain this nonlinear behaviour (Brantley et al., 1993; Shikama, 1998, 2006; Wallace et al., 1982; Wazawa et al., 1992). Both Wazawa et al. (1992) and Brantley et al. (1993) present models that explain the results of George and Stratmann (1952), and while they have some similarities, they have different ways of accounting for the fact that autoxidation of Mb has a maximum at low concentrations.

The aim of the present work is to couple a reasonably complete description of the redox chemistry of myoglobin in meat with the diffusion of oxygen. There are other processes that consume oxygen, such as mitochondrial respiration. We represent them by a single linear consumption term. We apply at the model from Brantley et al. (1993), and include diffusion and additional consumption which results in coupled reaction-diffusion equations. This is referred to as the extended Brantley model. We show that it is capable of predicting the formation of the sub-surface MMb layer. Furthermore, as an example, we apply the model to predict the oxygen and myoglobin concentrations in meat with a myoglobin concentration of $2.6 \cdot 10^{-4}$ M and pH between 5.4 and 5.6 comparable to a beef *longissimus dorsi* muscle at 5 °C (Sáenz et al., 2008).

To simplify the problem while keeping the important dynamical features, we model a single cut of meat in a one dimensional geometry. This is appropriate since we are interested in the outermost few millimeters of the meat which is the relevant length scale for the colour. In such a one dimensional model the dimensions of the meat, other than its thickness (10 mm), are irrelevant. Given a single cut of meat we make the further assumptions that diffusion is isotropic and homogeneous, and that the myoglobin is uniformly distributed in the meat. In reality a degree of anisotropy and inhomogeneity would be expected due to the fiber direction and meat structure (Aberle et al., 2012); handling these complications is left for future work. On the time scales studied here the diffusion of the myoglobin is too slow to be relevant with a diffusion constant of (in muscles (Moll, 1968)) about 0.05 mm^{2}h^{-1}. This is more than an order of magnitude smaller than that of oxygen (around 2.5 mm^{2}h^{-1}) (Chaix et al., 2014), thus, in the model presented here the different myoglobin forms do not diffuse. Also, in this initial modelling we let the oxygen concentration at the boundary be constant. Strictly, this corresponds to an infinitely large headspace with fixed partial pressure of oxygen. Measurements (Tørngren, 2016) show that the partial pressure of oxygen is approximately constant for the first 5–6 days after packaging, and the constant oxygen concentration assumption is valid in the time scale we study here.

2. Theory

2.1. Chemical model

2.1.1. Reversible oxygenation and irreversible oxidation

In this section we discuss the general chemistry behind myoglobin oxygenation and oxidation before focusing on the chemical model of Brantley et al. (1993). Before we discuss oxidation mechanisms we consider the reaction that is desirable, both physiologically and in the context of meat colour, namely oxygenation. The reaction is

$$MbO_2 \rightleftharpoons Mb + O_2, \quad K_d = \frac{[Mb][O_2]}{[MbO_2]}, \tag{1}$$
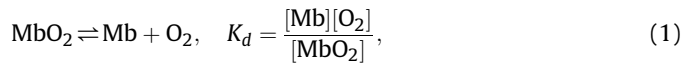
and is characterized by the equilibrium constant K_d. Equilibrium is reached on time scales of order 20–100 ms (Antonini and Brunori, 1971). As is common practice we use upper case K to represent equilibrium constants, and lower-case k to represent kinetic rate constants. Both in living muscle and in meat, Mb and MbO$_2$ undergo the process of autoxidation, producing metmyoglobin. At pH 7.2 and temperature 25 °C the first-order half-life of Mb is of order 10–100 h depending on the type of myoglobin (Shikama, 1998). In the living organism reducing enzymes allow reduction of MMb to Mb to maintain physiological function, and these are to a certain extent present in meat also, but in this work we characterize autoxidation in meat as irreversible. The large difference in time scales between reversible binding and irreversible oxidation is related to the nature of the surrounding protein matrix, and indeed evolution has selected the shape of Mb in order to reduce the rate of autoxidation while preserving the ability for reversible binding (Shikama, 2006). In the theoretical analysis and for numerical solutions it is convenient to exploit the time scale difference, and assume that reaction (1) is always in equilibrium. Then, from the equilibrium constant the fractions [Mb]/[Mb(II)] and [MbO$_2$]/[Mb(II)] are functions of K_d,

$$\frac{[Mb]}{[Mb(II)]} = \frac{K_d}{[O_2] + K_d} \tag{2}$$

$$\frac{[MbO_2]}{[Mb(II)]} = \frac{[O_2]}{[O_2] + K_d} \tag{3}$$

where [Mb(II)] represents the total concentration of myoglobin in its reduced form, whether oxygenated or not, that is

$$[Mb(II)] = [Mb] + [MbO_2]. \tag{4}$$

The mechanism for autoxidation of myoglobin and hemoglobin has been investigated thoroughly for decades, in particular by Shikama and coworkers and Olson and coworkers, see Alayash et al. (1998); Aranda et al. (2008); Brantley et al. (1993); Shikama (1998, 2006); Sugawara and Shikama (1980); Wazawa et al. (1992), but no definitive picture exists yet. Much work has involved inferring mechanisms from O_2 and pH dependence, and by comparing with mutant forms of myoglobin, for example by substituting the distal histidine residue that forms hydrogen bonds to O_2. More recently molecular simulations combining quantum and classical force fields have been used to shed light on the mechanism (Arcon et al., 2015).

2.1.2. Brantley model

Brantley et al. (1993) have proposed a mechanism that reproduces the results of George and Stratmann (1952), namely that the apparent oxidation rate of Mb(II) has a peak around 4 μM of

dissolved O_2. It is a combination of two pathways. One is unimolecular—a direct dissociation of a superoxide ion from the oxyform as suggested by Weiss (1964), the other is a bimolecular pathway based on a proposal by Wallace et al. (1982). It involves binding of a third species, a nucleophile, N, possibly water (Brantley et al., 1993), to deoxy-myoglobin. This then facilitates autoxidation with a rate proportional to both $[O_2]$ and [MbN]. The total reaction mechanism, including both oxidation pathways, is

$$MbO_2 \leftrightharpoons Mb + O_2 \tag{5}$$

$$MbO_2 \xrightarrow{k_{\mathrm{diss}}} MMb + O_2^- \tag{6}$$

$$Mb + N \underset{k_{-1}}{\overset{k_1}{\rightleftharpoons}} k_1 MbN \tag{7}$$

$$MbN + O_2 \xrightarrow{k_2} MMbN + O_2^- \tag{8}$$

Note that while O_2^- is very reactive it is assumed in the Brantley model to react with species that are irrelevant for this model, and that for both the bimolecular reactions (7) and (8), and the dissociation reaction, reaction (7), the net result is that one unit of O_2 oxidizes one unit of Mb(II). The reaction diagram can be seen in Fig. 1. With a steady state assumption for nucleophile, and assuming that the steady state value is small, an expression for the bimolecular contribution to the rate can be derived (Brantley et al., 1993; Wallace et al., 1982), giving an effective rate

$$r = \frac{k_1[N]k_2[O_2]K_d}{(k_{-1} + k_2[O_2])([O_2] + K_d)}[Mb(II)]. \tag{9}$$

For small $[O_2]$ it increases linearly with respect to $[O_2]$. For large $[O_2]$ the two factors in the denominator are both proportional to $[O_2]$, and therefore the overall rate decreases as $[O_2]^{-1}$. Brantley et al. (1993) make the further assumption that $k_{-1}k_2^{-1} \simeq K_d$, consistent with observations that the peak of the Mb oxidation rate occurs at $[O_2] = K_d$. MMbN has the same colour as MMb and therefore in this model is considered equivalent. This means that except for the equilibrium between Mb and MbO_2, the two different pathways that create MMb are independent of each other. The total effective autoxidation rate is therefore

$$r_{\mathrm{ox}} = \left(\frac{k_1[N][O_2]K_d}{([O_2] + K_d)^2} + \frac{k_{\mathrm{diss}}[O_2]}{[O_2] + K_d} \right)[Mb(II)]. \tag{10}$$

Viewed as functions of $[O_2]$, the first (bimolecular) term is where the maximum occurs; the second (unimolecular) term
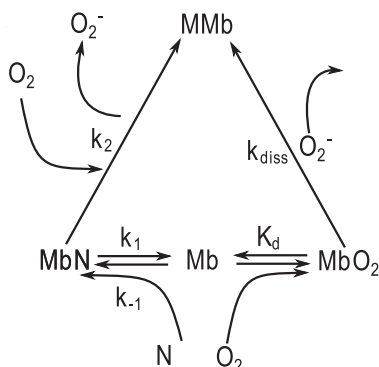
contributes a simple Michaelis-Menten type rate, saturating at a value k_{diss} for oxygen concentrations much higher than K_d. This value is also the limiting value of the whole expression at high $[O_2]$. Assuming that [N] is constant we define

$$k_b = k_1[N], \tag{11}$$

and we find that the maximum of k_{oxbi} is reached when $[O_2] = K_d$, with value $k_b/4$.

2.2. Other oxygen consuming processes

Oxygen is the driver of everything that happens in our model; as such we need to keep track of everything that could consume oxygen, such as mitochondria. A complete description of all oxygen consuming processes in meat is beyond the scope of this work, as such they will all be lumped together as one linear term (valid for sufficiently low O_2 concentration),

$$\left(\frac{d[O_2]}{dt} \right)_{\mathrm{con}} = -k_{\mathrm{con}}[O_2]; \tag{12}$$

k_{con} is the consumption rate constant.

2.3. Diffusion and elimination of fast time-scale

When adding a diffusion term we make two assumptions: (i) only the free oxygen can diffuse, or more precisely, it is the gradient of free oxygen that determines the mass flux (Fick's law); (ii) the equilibrium between MbO_2 and Mb in reaction (1) is very fast (Wazawa et al., 1992) compared to the other relevant time scales. The advantage of this is that it is not necessary to simulate the system at the shortest time scale, which would be computationally expensive, and here we wish to simulate time scales long compared with the oxygenation equilibrium. We therefore do not simply add a diffusion term to the dynamical equation for free oxygen. Rather, we take into account that as free oxygen diffuses, re-equilibration immediately occurs such that the equilibrium condition in reaction (1) is satisfied at all times. The result will be an effective diffusion term given by a non-linear function of the oxygen and Mb(II) concentrations. The non-linearity is the price we pay for removing the fast degree of freedom associated with reaction (1); in a numerical simulation it poses no problems.

Since the fast re-equilibration is relevant not just for diffusion, but also for chemical reactions involving oxygen let us consider more generally how the concentration of free oxygen changes as a result of processes affecting the total concentration of oxygen and the total concentration of Mb(II). We have from reaction (3)

$$[MbO_2] = \frac{[O_2]}{[O_2] + K_d}[Mb(II)], \tag{13}$$

and the total oxygen, which we denote $[O_2]_t$, can be given as a sum of the free and bound oxygen according to

$$[O_2]_t = [O_2]\left(1 + \frac{[Mb(II)]}{[O_2] + K_d} \right). \tag{14}$$

We invert this to get free oxygen as a function of the total oxygen and [Mb(II)]. Multiplying by the denominator gives

$$[O_2]_t([O_2] + K_d) = [O_2]([O_2] + [Mb(II)] + K_d). \tag{15}$$

This is a second degree polynomial for $[O_2]$ whose solutions are

Fig. 1. The chemical reaction mechanism in the Brantley model.

$$[O_2] = \frac{1}{2}\left([O_2]_t - [Mb(II)] - K_d \pm \sqrt{A}\right), \tag{16}$$

where

$$A = [O_2]_t^2 + [Mb(II)]^2 + K_d^2 + 2K_d[Mb(II)] + 2K_d[O_2]_t$$
$$- 2[O_2]_t[Mb(II)]. \tag{17}$$

To ensure a positive result we take the positive root. This gives the concentration of free oxygen as a function of the concentrations of total oxygen and Mb(II). Infinitesimal changes in $[O_2]_t$ and $[Mb(II)]$ then lead to a change in free $[O_2]$ given by

$$d[O_2] = \frac{\partial[O_2]}{\partial[O_2]_t}d[O_2]_t + \frac{\partial[O_2]}{\partial[Mb(II)]}d[Mb(II)]. \tag{18}$$

The first term can be evaluated as

$$\frac{\partial[O_2]}{\partial[O_2]_t} = \frac{1}{2}\left(1 + \frac{[O_2]_t + K_d - [Mb(II)]}{\sqrt{A}}\right) = \frac{1}{1 + \frac{K_d[Mb(II)]}{(K_d+[O_2])^2}}, \tag{19}$$

and the second term as

$$\frac{\partial[O_2]}{\partial[Mb(II)]} = \frac{-[O_2]}{[O_2] + K_d} \frac{1}{1 + \frac{K_d[Mb(II)]}{(K_d+[O_2])^2}}. \tag{20}$$

Equations (18)–(20) can now be used to write the change in free oxygen caused by the diffusion and chemical reaction processes whose effects on the total oxygen and Mb(II) content are known.

2.3.1. Diffusion

Consider diffusion of oxygen to or from a point during a time interval dt. We use a superscript "diff" to indicate changes in total and free oxygen due to diffusion. The change in total oxygen is given via Fick's law for the free oxygen as

$$d[O_2]_t^{diff} = D\frac{\partial^2[O_2]}{\partial x^2}dt. \tag{21}$$

Note the appearance of free oxygen in the second derivative term. Recall Mb(II) does not diffuse on the time scales we study, $d[Mb(II)]^{diff}=0$, and Eq. (18) becomes

$$d[O_2]^{diff} = \frac{D}{1 + \frac{K_d[Mb(II)]}{(K_d+[O_2])^2}}\frac{\partial^2[O_2]}{\partial x^2}dt. \tag{22}$$

This gives the appropriate diffusion term, where the diffusion constant D has been replaced by an effective diffusivity which is a non-linear function of $[O_2]$ and $[Mb(II)]$.

The diffusion term is to be added to the equation for the time-derivative of the free oxygen. Note that since the diffusion term is the only term involving length, the equations are invariant under a simultaneous rescaling of the diffusion constant and position co-ordinate. In other words, a change in the diffusion constant by a factor of two will yield solutions at a given time which are identical except for a rescaling in space by a factor $\sqrt{2}$. This is a feature of ordinary diffusion which is unaffected by integrating out of the fast degree of freedom.

2.3.2. Reactions

The fast equilibrium also effects the change in free oxygen due to chemical reactions. We use a superscript "reac" to indicate these changes to total and free oxygen. The treatment of this is similar to what was done for diffusion, except that now typically both

derivatives in Eq. (18) contribute. For example, in a reaction where one total oxygen unit and one Mb(II) unit are lost, we have $d[Mb(II)] = d[O_2]_t$ and the total change is

$$d[O_2]^{reac} = \left(\frac{\partial[O_2]}{\partial[Mb(II)]} + \frac{\partial[O_2]}{\partial[O_2]_t}\right)d[Mb(II)] \tag{23}$$

$$= \left(\frac{K_d}{[O_2] + K_d}\right)\frac{1}{1 + \frac{[Mb(II)]K_d}{(K_d+[O_2])^2}}d[Mb(II)]. \tag{24}$$

2.4. The extended model

Consider now the Brantley model, reactions (5)–(8). To obtain the dynamical equations where the fast degrees of freedom have been eliminated we include reaction and diffusion terms as discussed above. The reaction terms are determined from the law of mass action (Brantley et al., 1993). The change in oxygen concentration given by the law of mass action is the change in total oxygen concentration; it must be corrected using the procedure above to give the corresponding change in free oxygen under conditions of fast re-equilibration. This procedure gives

$$\frac{\partial[O_2]}{\partial t} = \frac{1}{1 + \frac{[Mb(II)]K_d}{(K_d+[O_2])^2}}\left(D\frac{\partial^2[O_2]}{\partial x^2}\right.$$
$$\left. - k_{con}[O_2] - \frac{[Mb(II)]K_d}{[O_2] + K_d}\left(\frac{k_1[N][O_2]K_d}{([O_2] + K_d)^2} + \frac{k_{diss}[O_2]}{[O_2] + K_d}\right)\right) \tag{25}$$

$$\frac{\partial[Mb(II)]}{\partial t} = -k_{diss}[MbO_2] - \frac{k_bK_d[O_2]}{([O_2] + K_d)^2}[Mb(II)] \tag{26}$$

$$\frac{\partial[MMb]}{\partial t} = k_{diss}[MbO_2] + \frac{k_bK_d[O_2]}{([O_2] + K_d)^2}[Mb(II)] \tag{27}$$

with

$$[MbO_2] = \frac{[Mb(II)][O_2]}{K_d + [O_2]} \quad \text{and} \quad [Mb] = \frac{[Mb(II)]K_d}{K_d + [O_2]}. \tag{28}$$

Note that the last two equations are algebraic, corresponding to the loss of the fast degree of freedom for binding oxygen to reduced myoglobin. The initial values are

$$t = 0: \quad [O_2] = S_{0_2}p_{O_2}\delta(x), \quad [Mb] = [Mb]_0, \quad [MMb] = 0,$$

where the concentration of oxygen is found from Henry's law, S_{0_2} is solubility of oxygen, p_{O_2} is the partial pressure of oxygen and $\delta(x)$ is the Dirac delta. Since the myoglobin forms do not diffuse it suffices to specify the boundary conditions for the concentration of oxygen; they are of mixed types of fixed and no-flux boundaries

$$x = 0: \quad [O_2] = S_{0_2}p_{O_2}, \quad \text{and} \quad x = L: \quad \left.\frac{\partial[O_2]}{\partial x}\right|_{x=L} = 0.$$

The dynamical equations are discretized in space through the finite difference approximation, and the dynamical equations are solved using Matlab's ode45 integrator which involves both 4th and 5th order Runge-Kutta steps with adaptive step-size (MATLAB, 2015). Choosing appropriate kinetic parameters (by kinetic is meant both chemical kinetic parameters and the diffusivity) is less straightforward; in the next section we describe how we attempt to identify the most appropriate values of the parameters. Table 1

Table 1
Most important model assumptions.

Physical Processes
Mb-forms immobile (diffusion zero)
Henry's law applies, $[O_2] = 0.7p_{O_2}k_H$

Chemical Processes
Mb and MbO$_2$ are in equilibrium
The Brantley model (Brantley et al., 1993) is applicable
No MMB reduction takes place
The super-oxide is not relevant for the problem

Biological Processes
No bacteria growth on meat surface
Mitochondria oxygen consumption is linear, $k_{con}[O_2]$

summarizes the important assumptions on which the model is made.

3. Results and discussion

3.1. Estimation of model parameters

In this section we describe how we determine the relevant parameters for the extended model and compare to data of Sáenz et al. (2008). We wish to determine the parameters for temperatures 20 °C and 5 °C both with a pH around 5.5. A simulation involves a specific kind of meat exposed to a specific MAP gas mixture at a specific temperature. For our purpose the relevant parameters characterizing of the meat are the myoglobin content and its pH; the relevant parameter characterizing of the gas mixture is the oxygen partial pressure, which is related to the equilibrium concentration in the meat via the solubility. In the next subsection we discuss our choice of myoglobin content and oxygen solubility. This is followed by extrapolation of the kinetic parameters for reversible and irreversible reactions of oxygen with myoglobin, and the diffusivity of oxygen, to the relevant pH (5.5) and temperatures (5 °C and 20 °C). Following this we compare to data by Sáenz et al. (2008) (temperature 20 °C); it will turn out that even a rough agreement requires significant corrections to one parameter, namely k_{con}. Finally we present model results for a typical meat-storage temperature, 5 °C.

3.1.1. Basic parameters: myoglobin content and oxygen solubility

To use the model we need to determine the concentration of myoglobin and the solubility of oxygen in meat. Since oxygen can react in many different ways in meat it is difficult to measure the true solubility of oxygen in meat. Chaix et al. (2014) estimated the solubility as $1.4 \cdot 10^{-8}$ mol kg^{-1} Pa^{-1} at 5 °C by assuming it to be equal to the oxygen solubility in water times the weight fraction of water in meat. The concentration of myoglobin depends on several factors such as type of animal, age of the animal and which cut of meat is used. Even if all these factors are the same there is still a large variation (Babji et al., 1989). For our work we choose a myoglobin content of 4.2 mg g^{-1} since this the myoglobin concentration in the experiments used in Sáenz et al. (2008), see Table 2.

3.1.2. Kinetic parameters extrapolated to relevant temperatures and pH

In this section we attempt to use literature data to determine the

Table 2
Oxygen solubility coefficient and initial myoglobin concentration.

S_{ox}	$1.4 \cdot 10^{-8}$ mol kg^{-1} Pa^{-1}
$[Mb(II)]_0$	$2.44 \cdot 10^{-4}$ mol

kinetic parameters appropriate for meat stored at 5 °C. We concentrate first on the parameters K_d, k_{diss}, k_{con} and D; the remaining chemical kinetic parameter k_b is discussed in the following subsection. Obtaining parameter values at the relevant temperature and pH is not straightforward, since only few measurements have been done on the autoxidation of myoglobin at low oxygen concentration, and none at temperatures around 5 °C. Furthermore the measurements that have been made are not necessarily from same species, and have often been at physiological pH, around 7, rather than that typical of fresh meat, pH around 5.5. We assume that unless data indicating otherwise is available that the temperature dependence of kinetic parameters can be described using the Arrhenius law,

$$\ln(k) = \frac{-E_a}{R}\frac{1}{T} + \ln(A) \tag{29}$$

This requires that we need at least 2 points to fit and extrapolate. For equilibrium constants we use the Van't Hoff equation,

$$\frac{\ln(K_2)}{\ln(K_1)} = \frac{-\Delta H}{R}\left(\frac{1}{T_2} - \frac{1}{T_1}\right), \tag{30}$$

which similar to the Arrhenius law involves an activation energy and requires two data points. There are no standard formulas representing pH dependence, and in fact the pH dependence of the oxidation rate of myoglobin is highly non-trivial (Shikama, 1998). Fortunately, there exist sufficient data to allow simple extrapolation. It is necessary, however, to assume the difference between species can be neglected. We take the three above-mentioned parameters one at a time.

Linear oxidation rate. We have from Brantley et al. (1993) that the linear reaction rate of sperm whale myoglobin is 0.051 h^{-1} at 37 °C and from Wazawa et al. (1992) that it is $8.1 \cdot 10^{-3}$ h^{-1} for 25 °C both at pH = 7. Assuming a Arrhenius temperature dependence Eq. (29) we use this to calculate a activation energy and find that $k_{diss} = 2.6 \cdot 10^{-4}$ h^{-1} at 5 °C and pH 7. To account for the pH difference we use data for bovine myoglobin from Sugawara and Shikama (1980) according to which changing from pH 7 to pH 5.5 increases k_{diss} by a factor which grows linearly with temperature, see Fig. 2. Fitting this data gives the relevant factor for 5 °C as 4.3 and for 20 °C as 6.7. For 20 °C and pH 5.5 we get $k_{diss} = 2.4 \cdot 10^{-2}$ h^{-1}, and we get for 5 °C and pH = 5.5 that $k_{diss} = 1.8 \cdot 10^{-3}$ h^{-1}. This value, corresponding to a time scale of several weeks, is too low for significant oxidation to occur during typical meat storage times of order one week. Therefore the contribution from the bimolecular term is essential for oxidation at low temperatures.

Oxygen dissociation constant. We have from Antonini and Brunori (1971) the activation enthalpy in the Van't Hoff equation, Eq. (30), that the dissociation reaction is −15 kcal mol^{-1}. The pH dependence is given via $-\Delta \log_{10} p_{\frac{1}{2}}\Delta pH^{-1} = 0.03$, where $p_{\frac{1}{2}}$ is the oxygen partial pressure at which $[MbO_2] = [Mb]$ (Antonini and Brunori (1971). We know from reaction (1) that $p_{\frac{1}{2}}$ is proportional to K_d meaning that

$$\frac{\Delta \log_{10} K_d}{\Delta pH} = -0.03 \tag{31}$$

The measured K_d is $1.0 \cdot 10^{-6}$ M at pH = 7.45 and a temperature of 20°. We find a K_d of $3.5 \cdot 10^{-7}$ M^{-1} for 5 °C and pH of 5.5, and a K_d of $1.2 \cdot 10^{-6}$ M^{-1} for 20 °C and pH of 5.5.

Oxygen diffusivity We have from Chaix et al. (2014) that the oxygen diffusivity in beef muscles is 1.8, 2.6, 3.0 mm^2 h^{-1} at 0, 5 and 10° C, respectively. Using the Arrhenius equation, we get $A = 2.5 \cdot 10^6$ mm^2 h^{-1} and $E_a = 32$ kJ mol^{-1} giving us a diffusion
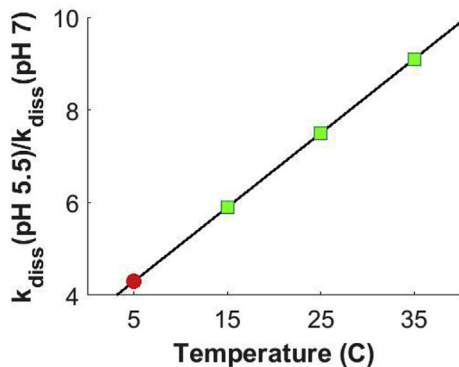
Fig. 2. k_{diss}(pH 5.5)/(k_{diss}(pH 7) as a function of temperature. Squares are data points from Sugawara and Shikama (1980); line represents the best linear fit to the data. The circle is the extrapolated data point for 5 °C.

Fig. 3. First attempt to compare extended Brantley model with data of Sáenz et al. (2008) at $t = 2$ h. The rate constant k_b for the bimolecular reaction has been set to the value 7.4 h^{-1}, while the other parameters is one as given in Table 3. Concentration profiles are normalized to the maximum values in the sample–for the different Mb species this is simply the initial concentration of Mb; for oxygen it is the fixed value applied at the boundary $x = 0$ corresponding to a partial pressure of 20% of atmospheric pressure. The concentrations have been normalized such that the sum of the concentrations of all the myoglobin forms is one at each point. The concentration of free oxygen has been normalized so it is one at the meat surface.

constant of 6.0 mm^2 h^{-1} at 20 °C.

Oxygen consumption constant. While we do not have a directly measured value for k_{con}, an approximate value can be inferred from measurements by Tang et al. (2005) of the oxygen consumption in mixtures of mitochondria and Mb at pH 5.6 and 25°C. Their data shows roughly exponential decay of oxygen concentration, i.e., a first order kinetic model with respect to oxygen concentration, with a time constant of 0.1–0.2 min^{-1} or 6–12 h^{-1}, depending on the concentration of mitochondria. Furthermore Abele et al., (2002) measured that the oxygen consumption rate decreases by a factor between 2 and 3 when the temperature is decreased from 20°C to 5°C. Initially we choose the values 10 h^{-1} and 4 h^{-1} for 20° C and 5°C. This gives us the parameters in Table 3.

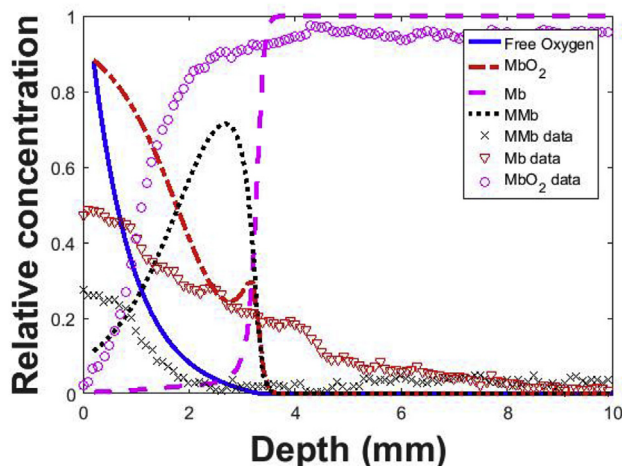### 3.1.3. Fitting the extended Brantley model to data of Sáenz et al.

For the Brantley model there is one parameter in addition to those just discussed, namely k_b, the rate constant for the bimolecular oxidation pathway. The only data point available is from Brantley et al. (1993) for sperm whale myoglobin, $k_b = 1.1$ h^{-1} for pH 7 and 37 °C. It is presumably different at the temperatures and pH of interest to us, but we start by considering this value along with the parameters in Table 3 for 20 °C. Running the simulation up to time $t = 2$ h gives the profiles shown in Fig. 3 curves. The corresponding data from Sáenz et al., (2008) are shown as points. There are clearly large differences between the model output and the data. The three most salient are: (i) the locations of the rise of deoxy-Mb from 0 to 1 (i.e. 100% of the initial concentration of Mb) and the peak in MMb are too far from the meat surface by a factor of order 2–3, suggesting the diffusion constant has been overestimated or the consumption constant has been underestimated. (ii) The width of the transition from MbO$_2$ to Mb is much smaller for the model than for the experimental data. The peak concentration and the total (integrated) amount of MMb are too large, presumably due to an overestimate of k_b.

We can obtain partial agreement with the experimental data by increasing k_{con} by a factor of 10, and choosing k_b=1.2 h^{-1}; see Fig. 4 for $t = 2$ h and Fig. 5 for $t = 8$ h. k_{con} is chosen so that Mb curve is

Table 3
Extrapolated parameter values used in the first simulation (Fig. 3) of the extended model for pH = 5.5 and two temperatures 5 °C and 20 °C.

	20 °C	5 °C
K_d	$1.2 \cdot 10^{-6}$ M	$3.5 \cdot 10^{-7}$ M
k_{diss}	$2.4 \cdot 10^{-2}$ h^{-1}	$1.8 \cdot 10^{-3}$ h^{-1}
D	6.0 mm^2 h^{-1}	2.6 mm^2 h^{-1}
k_{con}	10 h^{-1}	4 h^{-1}

close to the data, and k_b is chosen so that the integral under the peak is the same at 2h. This value is close to the value 1.1 h^{-1} reported by Brantley et al. (1993) for T =37°C and pH 7. The agreement here is reasonable given the simplicity of the model (i.e. that it is one-dimensional, homogeneous, and not all of the chemistry has been included). Instead of increasing k_{con} we could have decreased D by the same factor, giving almost the same effect. The data does not allow us to uniquely determine both parameters. We choose to keep our initial value for D, but it should be noted that it was based on literature data compiled by Chaix et al. (2014). The values there came from Zaritzky and Bevilacqua (1988) who did not measure them; rather they extrapolated a value for 37°C to lower temperatures using the Wilke-Chang equation with the viscosity of water, thus some uncertainty in the value of D can be expected. On the other hand a factor of 10 change in k_{con} seems not too unreasonable given that this term is a fairly crude way to model all the other oxygen consuming processes, and given the uncertainty of mitochondrial concentration. Part of the discrepancy from our model compared to the data from Sáenz et al. (2008) is that the data is an average over the transverse direction of measurements in a broad piece of meat. Variations of meat structure in this direction lead to broadening of the averaged profiles. We note that there are also difficulties in determining, or even defining, the oxygen solubility in a complex system where oxygen can react with many components Chaix et al. (2014). More data is needed to reduce the uncertainty in these parameters; for the rest of the analysis we keep the solubility as given in Chaix et al. (2014). Almost no matter the exact value of k$_{con}$, the model predicts a red surface colour and a brown region inside the meat. This contrasts the experimental data from Sáenz et al. (2008), where the brown colour is visible on the meat surface.

One feature of the experimental data that the model cannot reproduce is the very broad MbO$_2$ profile. The decay region is much wider than the transition region for Mb. It is not clear why this is; possible reasons include inhomogeneity of the Mb concentration or an initial presence of oxygen in the sample (although Sáenz et al. (2008) took care to ensure the initial state was as oxygen-free as possible). It is not clear how the relative concentrations given by Sáenz et al. (2008) are calculated, but they do not add up to unity or
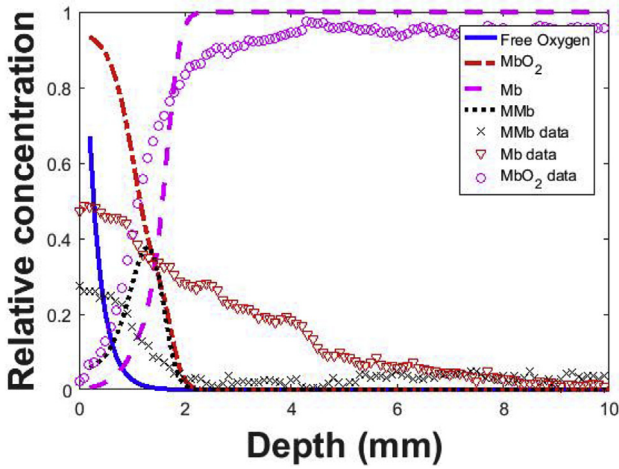
Fig. 4. Comparison of experimental data with extended Brantley model using parameters from Table 4, at 20 °C and time $t = 2$ h. Partial pressure of O_2 is 20% of atmospheric pressure. The concentrations have been normalized such that the sum of the concentrations of all the myoglobin forms is one at each point. The concentration of free oxygen has been normalized so it is one at the meat surface.
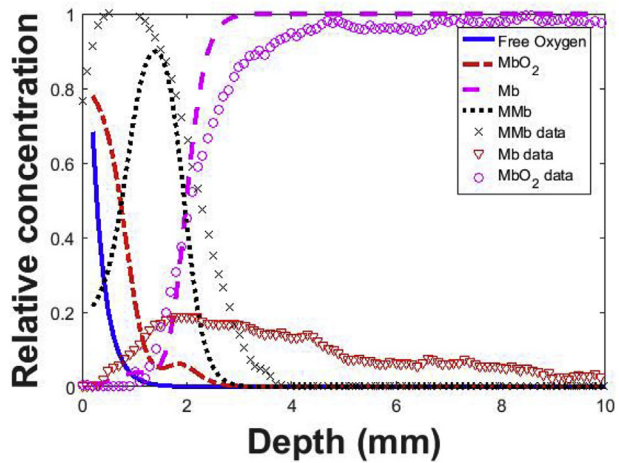
Fig. 5. Comparison of experimental data with extended Brantley model using parameters from Table 4, at 20 °C and time $t = 8$ h. Partial pressure of O_2 is 20% of atmospheric pressure. The concentrations have been normalized such that the sum of the concentrations of all the myoglobin forms is one at each point. The concentration of free oxygen has been normalized so it is one at the meat surface.

any constant value, which suggests some degree of inhomogeneity. Another possible reason could be the presence of reducing processes which are not included in our extended model. Further experimental work should be done to see if this broad decay is a real feature or an experimental artefact.

3.2. Application of extended brantley model to typical meat storage conditions

Finally, we apply the extended Brantley model to a typical meat storage temperature 5 °C. There is a challenge in adjusting the parameter k_b to the lower temperature—for simplicity we assume the same activation energy as for k_{diss}, which yields a value $k_b = 0.07$ h^{-1} at 5°C. Because of the parameter uncertainty, we are interested in the qualitative behaviour of the model; we cannot make definite quantitative predictions for real systems. We are particularly interested in studying how changes in the partial pressure of oxygen affect the formation of MMb. Using the

parameters in Table 4 we plot the MMb profile for a series of different oxygen pressures in Fig. 6 after 24 h of storage. The main effect of increasing oxygen pressure is to push the MMb peak slightly inwards, i.e. deeper into the meat. The effect is rather small, though; in fact it depends nearly logarithmically on the oxygen partial pressure as can be seen in the figure inset. This logarithmic dependence can explained in terms of two effects: (1) The oxygen profile relatively quickly approaches the exponential form $[O_2](x) = [O_2]_0 \exp(-\sqrt{k_{con}/D} x)$ which is the long-time limiting profile when no myoglobin oxidation takes place; (2) the oxidation rate peaks at the location x_{ox} where the oxygen concentration has a particular (low) value c_1, that is $[O_2](x_{ox}) = c_1$. It follows that $x_{ox} = \sqrt{D/k_{con}} \ln([O_2]/c_1)$, i.e. the location of the peak in MMb production is proportional to the logarithm of the boundary concentration and thus of the partial pressure of oxygen in the headspace. The higher the oxygen pressure the more the outermost layer is dominated by the red oxymyoglobin, making the meat look more desireable. The total amount of MMb generated is relatively insensitive to the oxygen pressure. The deeper location of MMb at higher is consistent with observations of stored meat (Aberle et al., 2012) and therefore shows that the extended model can reasonably represent the interplay between diffusion, reversible oxygenation and irreversible oxidation in stored fresh meat.

4. Conclusion

In this paper we have made a nonlinear reaction diffusion model that combines diffusion of oxygen, a general linear oxygen consumption term, reversible binding of oxygen to myoglobin, and irreversible oxidation of myoglobin in fresh meat. The dynamics of

Table 4
Parameter values adjusted by fitting to data of Sáenz et al. (2008) and used in the simulation of the Brantley model.

	20 °C	5 °C
K_d	$1.2 \cdot 10^{-4}$ M	$3.6 \cdot 10^{-5}$ M
k_{diss}	$2.3 \cdot 10^{-2}$ h^{-1}	$1.3 \cdot 10^{-3}$ h^{-1}
D	6 mm^2 h^{-1}	2.6 mm^2 h^{-1}
k_b	1.2 h^{-1}	0.07 h^{-1}
k_{con}	100 h^{-1}	40 h^{-1}
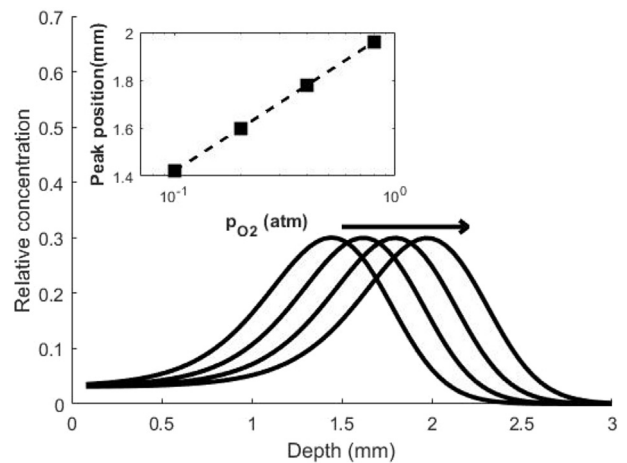
Fig. 6. Application of extended Brantley model to meat storage at 5 °C. The curves show MMb profiles at 24 h for increasing oxygen partial pressure at the boundary, from left to right 10%, 20%, 40% and 80%. The inset shows the location of the peak MMb concentration as a function of the partial pressure of oxygen on a logarithmic axis, along with a linear fit as a guide to the eye.

reversible binding take place on relatively short time scales, which we have exploited allowing us to take longer time steps in our numerical integration procedures, of order minutes rather than seconds. This is achieved mathematically by modifying the dynamical equations so that the effective diffusion coefficient becomes a non-linear function of oxygen concentration and Mb(II) concentration. A chemical model for the oxidation of Mb, due to Brantley et al. (1993) has been considered. For the Brantley model extended with diffusion and oxygen consumption, parameters for 20 °C and 5 °C were extrapolated from literature values. The model output was then compared to data of Sáenz et al. (2008) which consists of temporally and spatially resolved concentration profiles for Mb, MbO_2 and MMb at 20 °C. Some features of the experimental data cannot be matched by the model such as oxidizing the first millimetre of the meat, or the long tail of MbO_2. The reason for this discrepancy is not clear but can be the result of additional chemical processes. Extrapolating down to 5 °C, we used the model to study the effect of different partial pressures of oxygen on the degree and location of met-myoglobin formation, showing that high oxygen pressure pushes the region of high-MMb deeper into the meat, this shift is proportional to the logarithm of the oxygen concentration.

Progress will require both continued development of the model and more experimental data. In order to make the model more realistic and useful for predicting shelf-life we plan to expand the model in the following four ways: (i) Properly model it as a MAP system, i.e. with a limited headspace, (ii) include bacterial growth on the meat surface, (iii) introduce a MMb reducing mechanism, and (iv) take meat structure and inhomogeneity into account. Regarding data, two kinds are needed: (1) more measurements of individual kinetic parameters such as k_{diss} and K_d at relevant temperatures and pH, and for a variety of species; (2) more measurements like those of Sáenz et al. (2008) yielding temporally and spatially resolved information on diffusion, oxygenation, oxygen consumption and oxidation. The latter kind of data is essential, for example, to determine the oxygen diffusivity D, which cannot be determined in meat without taking reactions into account (Chaix et al., 2014); fitting a dynamical model such as the ones we have presented here to temporally and spatially resolved data is potentially a better way to get a proper estimate of the diffusivity.

Compliance with ethical standards

Conflict of interest

The authors declare that they have no conflict of interest.

Compliance with ethics requirements

This article does not contain any studies with living human or animal subjects.

Acknowledgements

References

Abele, D., Heise, K., Pörtner, H., Puntarulo, S., 2002. Temperature-dependence of mitochondrial function and production of reactive oxygen species in the intertidal mud clam *Mya arenaria*. J. Exp. Biol. 205 (4), 1831—1841.

Aberle, E.D., Forrest, J.C., Gerrard, D.E., Edward, W.M., 2012. Principles of Meat Science. W. H. Freeman.

Alayash, A.I., Ryan, B.A.B., Eich, R.F., Olson, J.S., Cashon, R.E., 1998. Reactions of sperm whale myoglobin with hydrogen peroxide. J. Biol. Chem. 274 (4), 2029—2037.

Antonini, E., Brunori, M., 1971. Hemoglobin and Myoglobin in Their Reactions with Ligands. North-Holland.

Aranda, R.I., Cai, H., Worley, C.E., Levin, E.J., Li, R., Olson, J., Phillips, G.N.J., Richards, M.P., 2008. Structural analysis of fish versus mammalian hemoglobins: effect of the heme pocket environment on autooxidation and hemin loss. Proteins 75, 203—217.

Arcon, J.P., Rosi, P., Petruk, A.A., Marti, M.A., Estrin, D.A., 2015. Molecular mechanisms of myoglobin autoxidation: insights from computer simulations. J. Phys. Chem. B 119, 1802—1813.

Babji, A.S., Ooi, P., Abdulah, A., 1989. Determination of meat content in processed meats using currently available methods. Pertanika 12 (1), 33—41.

Brantley Jr., R.E., Smerdon, S.J., Wilkinson, A.J., Singleton, E.W., Olson, J.S., 1993. The mechanism of autooxidation of myoglobin. J. Biol. Chem. 268, 6995—7010.

Chaix, E., Guillaume, C., Guillard, V., 2014. Oxygen and carbon dioxide solubility and diffusivity in solid food matrices: a review of past and current knowledge. Compr. Rev. Food. Sci. Food Saf. 13 (3), 261—286.

George, P., Stratmann, C.J., 1952. The oxidation of myoglobin to metmyoglobin by oxygen. Biochem. J. 51, 418—425.

MATLAB, 2015. Version 8.6.0 (R2015b). The MathWorks Inc., Natick, Massachusetts.

McMillin, K.W., 2008. Where is MAP Going? A review and future potential of modified atmosphere packaging for meat. Meat Sci. 80 (1), 43—65.

Moll, W., 1968. The diffusion coefficient of myoglobin in muscle homogenate. Pflügers Arch. 299, 247—251.

Owusu-Apenten, R., 2004. Introduction to Food Chemistry. CRC Press.

Riva, M., Sinelli, N., Franzetti, L., Torri, L., Limbo, S., 2009. Predictive modeling of the freshness of minced beef meat stored in MAP at different temperatures. Ital. J. Food Sci. 21, 14—18.

Sáenz, C., Hernández, B., Alberdi, C., Alfonso, S., Dineiro, J.M., 2008. A multispectral imaging technique to determine concentration profiles of myoglobin derivatives during meat oxygenation. Eur. Food Res. Tech. 227 (5), 1329—1338.

Shikama, K., 1998. The molecular mechanism of autoxidation for myoglobin and hemoglobin: a venerable puzzle. Chem. Rev. 4, 1357—1373.

Shikama, K., 2006. Nature of the FeO_2 bonding in myoglobin and hemoglobin: a new molecular paradigm. Prog. Biophys. Mol. Bio. 91, 83—162.

Sugawara, Y., Shikama, K., 1980. Autoxidation of native oxymyoglobin. Eur. J. Biochem. 110, 241—246.

Tang, J., Faustman, C., Hoagland, T.A., Mancini, R.A., Seyfert, M., Hunt, M.C., 2005. Postmortem oxygen consumption by mitochondria and its effects on myoglobin form and stability. J. Agr. Food Chem. 53 (4), 1223—1230.

Tørngren, M.A., 2016. Private Communication.

Wallace, W., Houtchens, R., Maxwell, J., Caughey, W., 1982. Mechanism of autoxidation for hemoglobins and myoglobins - promotion of superoxide production by protons and anions. J. Biol. Chem. 257 (9), 4966—4977.

Wazawa, T., Matsuoka, A., Tajima, G., Sugawara, Y., Nakamura, K., Shikama, K., 1992. Hydrogen peroxide plays a key role in the oxidation reaction of myoglobin by molecular oxygen. J. Biochem. 63, 544—550.

Weiss, J.J., 1964. Nature of the iron—oxygen bond in oxyhæmoglobin. Nature 202, 83—84.

Wikström, F., Williams, H., Verghese, K., Clune, S., 2014. The influence of packaging attributes on consumer behaviour in food-packaging LCA studies : a neglected topic. J. Clean. Prod. 73, 100—108.

Zaritzky, N.E., Bevilacqua, A.E., 1988. Oxygen diffusion in meat tissues. Int. J. Heat. Mass Tran. 31 (5), 923—930.